

Ordering phenomena in C₆₀-tetraphenylphosphonium bromide

 P. Launois^{1,a}, R. Moret¹, N.-R. de Souza¹, J.A. Azamar-Barrios^{2,b}, and A. Pénicaud²
¹ Laboratoire de Physique des Solides^c, bâtiment 510, Université Paris-Sud, 91405 Orsay Cedex, France

² Centre de Recherche Paul Pascal, Université de Bordeaux I, avenue Schweitzer, 33600 Pessac, France

Received 3 November 1999

Abstract. The fulleride salt C₆₀-tetraphenylphosphonium bromide is investigated as a function of temperature by single crystal X-ray diffuse scattering and diffraction. At room temperature, the C₆₀ orientational disorder is found to be more complex than previously expected. Moreover, a structural phase transition, due to the C₆₀ orientational ordering, is evidenced around 120 K. Its relation with the stabilization of a static Jahn-Teller effect is discussed.

PACS. 61.10.Eq X-ray scattering (including small-angle scattering) – 61.10.Nz Single-crystal and powder diffraction – 61.48.+c Fullerenes and fullerene-related materials

1 Introduction

The C₆₀ molecule has a strong electron affinity and numerous C₆₀-reduced solids have been synthesized. We cite, as an example, the doped fullerides, with three alkali per C₆₀, whose superconductivity was discovered in 1991, which are the highest-*T_c* organic superconductors [1]. Another intensively studied fullerene salt is TDAE. C₆₀, which is ferromagnetic below 16 K [2], the highest transition temperature known for all organic compounds. However, the understanding of the microscopic mechanisms responsible for the remarkable properties of the fullerene derivatives is still very incomplete, partly because of the scarcity of single crystals.

The icosahedral C₆₀ molecule has a three-fold degenerate (*t_{1u}*) lowest unoccupied molecular orbital. For C₆₀ anions, static or dynamic Jahn-Teller effects are expected to occur. In the static case, the degeneracy of the *t_{1u}* level is lifted by the electron-phonon interactions, the energy splitting being accompanied by a molecular deformation: the Jahn-Teller distortion [3–5]. It has been proposed that Jahn-Teller effects may play a key role in the understanding of the electronic properties of the alkali-metal doped fullerenes, in the fulleride superconductivity or ferromagnetism [6]. However, electron addition on the large C₆₀ molecule would result in very small distortions (typically, in C₆₀[−], one expects displacements of about 0.01 Å for only 20 atoms out of 60 [5]). Thus, direct structural observations of these distortions are rare [7, 8].

C₆₀-tetraphenylphosphonium halides were the first fulleride salts to be synthesized. They are stable in air and

were obtained in powder form in 1991 [9]. Two years later, they were shown to form single crystals by electrocrystallization [10]. Isostructural salts of general formula [Ph₄P⁺]₂[C₆₀[−]][X[−]]_{*x*}[Cl[−]]_{1−*x*}, with Ph = C₆H₅ and X = Cl, Br or I have been synthesized [10–12]. They have been thoroughly studied by X-ray diffraction [10–12], electron spin resonance (ESR) [9, 13–17], calorimetry [17], nuclear magnetic resonance [18], infrared [11(b), 19, 20] and Raman [21] spectroscopies. Their structure has been determined independently by Pénicaud *et al.* [10] and by Bilow and Jansen [11]. The space group at room temperature is I4/m, with unit cell parameters *a* = *b* ~ 12.5 Å and *c* ~ 20.3 Å. The halogen ions are located at the origin of the unit cell, the tetraphenylphosphonium ions are located at (0, 1/2, 1/4) and the fullerene ions around 4/m centers at (0, 0, 1/2). The structure is a distorted CsCl-type structure where Cs⁺ is replaced by (Ph₄P)⁺ and where Cl[−] is alternatively replaced by an halogen or a fullerene ion. The Ph₄P⁺ cations form a host lattice stabilized by multiple phenyl embraces [22]. The C₆₀[−] anions are surrounded by eight Ph₄P⁺ cations and are well separated from each other. C₆₀-tetraphenylphosphonium halide salts are thus model systems to study C₆₀ monoanions in the solid state. Moreover, an interesting orientational property of these salts has been evidenced by the early structural studies [10, 11]. The molecule being located on a 4/m center with a two-fold axis parallel to the four-fold crystal axis *c*, it can take two orientations, related by a 90° rotation about the *c* axis, with equal probability [10, 11] (merohedral disorder). Actually, it appears that several (48 out of 60) C atoms on a molecule are close to other C atoms on the rotated molecule (Fig. 1). This is a further difficulty in view of direct structural investigations of the Jahn-Teller distortion. On the other hand, strong indications for a Jahn-Teller effect have been

^a e-mail: launois@lps.u-psud.fr

^b *Permanent address:* Cinvestav-Mérida, apdo postal 73 Cordemex, 97310 Mérida, Yuc., México

^c UMR 8502 du CNRS

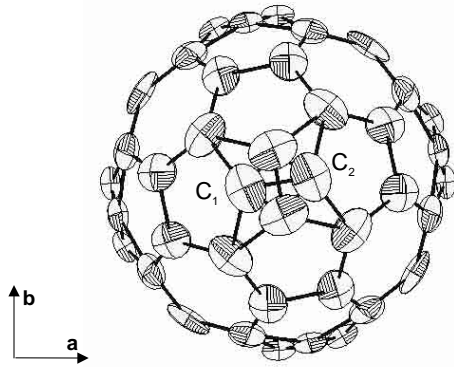


Fig. 1. Refined atomic positions and thermal ellipsoids for the C_{60} molecule at room temperature (I4/m space group). Interatomic bonds are drawn to facilitate visualization. The atoms C_1 and C_2 belong to the same C_{60} molecule. Two molecule orientations, related by a 90° rotation around the axis c , are found. C_1 and C_2 are well separated from the equivalent atoms on the rotated molecule, but 48 atomic positions out of 60 are not resolved and appear superimposed for the two molecule orientations.

provided by ESR [14,23] and by far-infrared studies [20]. These measurements have found changes in the molecular Landé factor of the fullerene or splitting of C_{60}^- vibrational modes, in connection with a symmetry lowering. In this paper we present a study of the X-ray diffuse scattering in C_{60} -tetraphenylphosphonium bromide as a function of temperature together with the results of a new low temperature structural determination. We discuss the Jahn-Teller effect in C_{60} -tetraphenylphosphonium halide salts in relation with the orientational ordering.

2 Experimental results: X-ray diffraction and diffuse scattering

$[\text{Ph}_4\text{P}^+]_2[\text{C}_{60}^-][\text{Br}^-]_x[\text{Cl}^-]_{1-x}$ single crystals were grown by electrocrystallization [10,23]. In the electrocrystallization procedure, C_{60} and $[\text{Ph}_4\text{P}][\text{Br}]$ were dissolved in toluene-dichloromethane, which was in fact also a source of chlorine [12], thus explaining the mixed formulae $[\text{Br}^-]_x[\text{Cl}^-]_{1-x}$. Elemental analysis performed on 10 mg of material gave $x \approx 0.42$ [23]. Diffraction data were obtained on single crystals of typical size $0.2 \times 0.25 \times 0.35 \text{ mm}^3$. Their analysis gives information about the average structure. X-ray diffuse scattering is usually more extended than Bragg scattering and its intensity is weaker. The X-ray diffuse scattering experiments have thus been performed on larger crystals of typical size $2 \text{ mm}^2 \times 0.1 \text{ mm}$. The diffuse scattering gives information about disorder or local order.

The crystals used to measure the diffuse scattering were first characterized at room temperature using the precession technique, which gives undistorted diffraction patterns of selected reciprocal planes. As an example, the measured diffraction pattern for $l = 0$ is shown in Figure 2a. It can be compared with that calculated

using the structural model of references [10,11] (Fig. 2b). The observed and calculated intensity distributions of the $(h, k, 0)$ reflections appear to be in good agreement.

The monochromatic fixed-crystal fixed-film technique was employed to detect the weak diffuse scattering signal between the Bragg peaks, and to follow its evolution as a function of temperature. $\text{CuK}\alpha$ radiation ($\lambda = 1.5418 \text{ \AA}$) was selected by reflection on a doubly-bent graphite monochromator. The crystal was placed in an evacuated chamber to remove air scattering. The diffuse scattering patterns were recorded on cylindrical ($\Phi = 60 \text{ mm}$) imaging plates or films. The low temperature experiments were performed using a cryocooler and the crystal was glued to the sample holder with varnish. Note that the temperature was measured on the cold end of the sample holder so that the actual crystal temperature was probably higher than the measured one.

Broad diffuse scattering modulations are clearly visible at room temperature, as shown in Figures 3a and 4a. The diffuse scattering intensity varies slowly in reciprocal space and its modulations extend over several Brillouin zones. Because the width of diffuse scattering intensity maxima are roughly proportional to the inverse of the correlation lengths in direct space, this indicates that the diffuse intensity is a signature of random disorder (or at least of very short-range correlations). The structure refinements (using the Bragg peak intensities) together with elemental analyses have identified two types of disorder: i) orientational disorder of the C_{60} molecules [10,11], ii) substitutional disorder between Cl^- and Br^- [12,23]. The diffuse intensity for the substitutional disorder is given by the Laue formula [24]:

$$I_D(\mathbf{Q}) \propto Nx(1-x) |f_{\text{Cl}^-}(Q) - f_{\text{Br}^-}(Q)|^2, \quad (1)$$

where \mathbf{Q} is the scattering wave vector, Q is its modulus, N is the number of unit cells and where f_{Cl^-} and f_{Br^-} are the X-ray form factors for the Cl^- and Br^- ions. This diffuse scattering intensity is a slowly decreasing function of the wave-vector, so that it does not account for the diffuse modulations in Figure 3a or in Figure 4a. The diffuse scattering for two differently oriented molecules randomly distributed on lattice sites can also be treated with a similar formalism [25]. For two possible orientations with equal probabilities, it reads:

$$I_D(\mathbf{Q}) \propto \frac{N}{4} |F_1(\mathbf{Q}) - F_2(\mathbf{Q})|^2, \quad (2)$$

where $F_1(\mathbf{Q})$ and $F_2(\mathbf{Q})$ are the form factors of the C_{60} molecule in its two orientations (Fig. 1). Note that the C_{60} molecular form factors exhibit a non-monotonous dependence with the wave-vector \mathbf{Q} (in contrast to the ionic form factors) so that pronounced diffuse scattering modulations are expected in this case. The diffuse scattering calculated from (Eq. (2)) for the two C_{60} orientations deduced from the structural analyses is shown in Figure 3b. It appears that the calculated and measured diffuse scattering do not agree, the calculated diffuse scattering distribution presenting fewer and more localized maxima. Note that strong diffuse scattering modulations are visible in

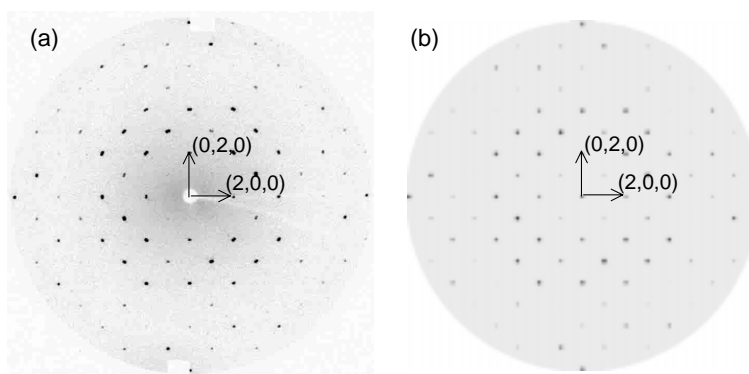


Fig. 2. Precession photograph of the $l = 0$ plane, exhibiting a four-fold symmetry. (a) Experiment: imaging plate, CuK α radiation ($\lambda = 1.5418 \text{ \AA}$); (b) simulation from the structural model of references [10,11].

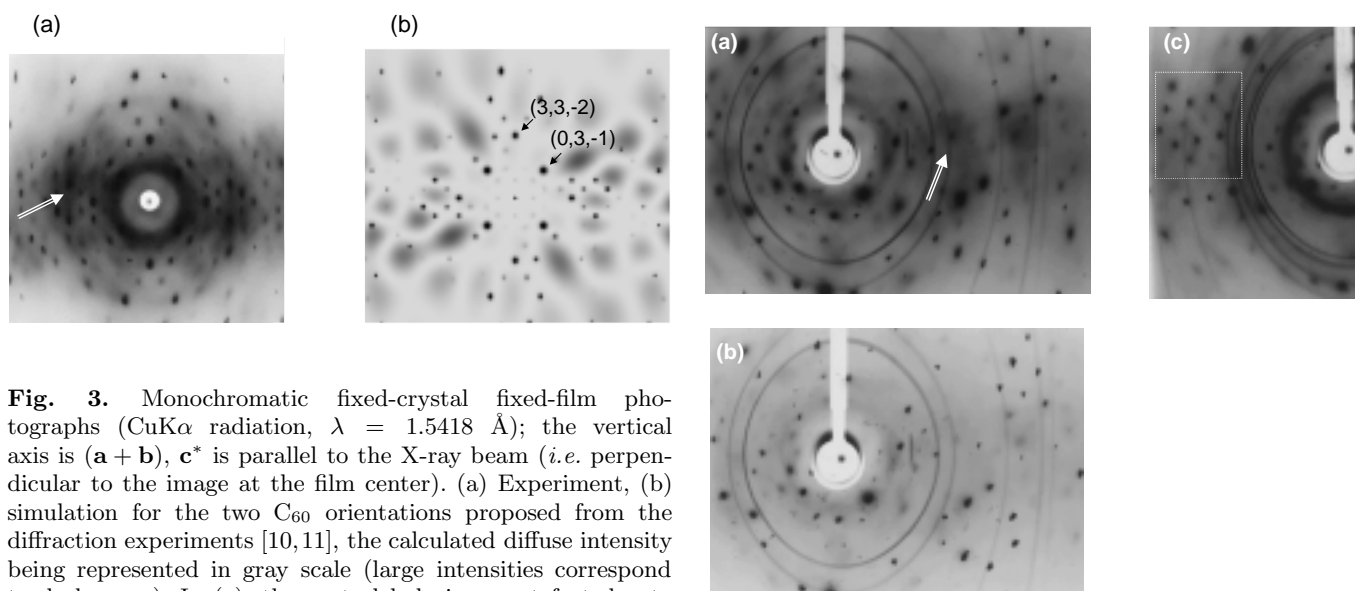


Fig. 3. Monochromatic fixed-crystal fixed-film photographs (CuK α radiation, $\lambda = 1.5418 \text{ \AA}$); the vertical axis is $(\mathbf{a} + \mathbf{b})$, \mathbf{c}^* is parallel to the X-ray beam (*i.e.* perpendicular to the image at the film center). (a) Experiment, (b) simulation for the two C₆₀ orientations proposed from the diffraction experiments [10,11], the calculated diffuse intensity being represented in gray scale (large intensities correspond to dark areas). In (a), the central halo is an artefact due to the sample holder. The double-arrow points toward a strong diffuse scattering area around 3.3 \AA^{-1} .

Figure 3a for values of the scattering vector modulus close to 3.3 \AA^{-1} . This is the position of the first diffuse halo characteristic of the orientational molecular disorder in the high temperature phase of pure C₆₀ [26-28]. One may thus infer that an important part of the diffuse scattering in C₆₀-tetraphenylphosphonium bromide is due to some C₆₀ orientational disorder, even though this disorder is more complex than that deduced from the structural refinements in references [10,11].

It is worth pointing out also that diffuse lines are observed in some regions of the diffuse scattering patterns. These lines join Bragg reflections along directions of the type $\mathbf{b}^* + \mathbf{c}^*$ ($\mathbf{a}^* + \mathbf{c}^*$) and they are clearly visible in Figure 4c. Such diffuse lines are the signature for stacking disorder of (011), (01 $\bar{1}$), (101) and (10 $\bar{1}$) planes or layers in the structure. The origin of the disorder is not yet fully understood but an interesting feature can already

Fig. 4. Monochromatic fixed-crystal fixed-film photograph (CuK α radiation, $\lambda = 1.5418 \text{ \AA}$): (a) $T = 285 \text{ K}$, (b) $T = 35 \text{ K}$, (c) $T = 115 \text{ K}$ (exposure times are 24, 24 and 32 hours, respectively). The double-arrow points toward a 3.3 \AA^{-1} strong diffuse scattering area. In the dotted area in (c) diffuse lines joining Bragg reflections and in the shape of lozenges run along directions of the type $\mathbf{a}^* + \mathbf{c}^*$ and $\mathbf{b}^* + \mathbf{c}^*$. The central halo and the sharp rings are artefacts due to diffraction from the sample holder.

be noted: the (011)-type planes are homopolar planes of each constituent of the salt, with the following sequence: Br⁻/Cl⁻, Ph₄P⁺, C₆₀⁻, Ph₄P⁺, and so on, as seen in Figure 5.

Comparing Figures 4a and 4b one observes that the broad diffuse scattering intensity strongly decreases with temperature. This diffuse scattering decreases most between room temperature and 110 K; below 110 K, it is too weak to be measured. The diffuse line intensities also

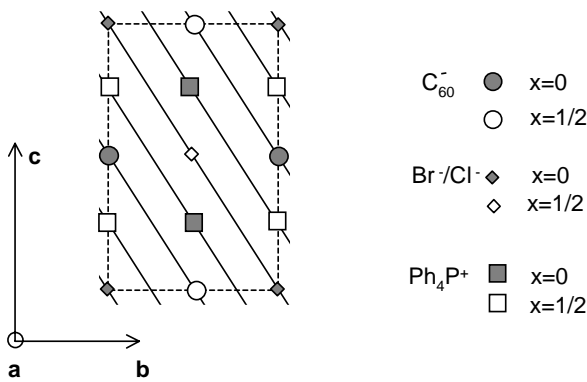


Fig. 5. Schematic representation of the (011) homopolar planes (solid lines).

decrease with temperature. The overall decrease of diffuse scattering with temperature indicates a dramatic reduction of the disorder. However, since the origin of the diffuse scattering is not fully clarified, the understanding of its temperature dependence remains incomplete.

In contrast to the diffuse scattering evolution, the fixed-crystal fixed-film photographs reveal no significant change in the Bragg peak reflection pattern, down to 35 K. In particular no supplementary Bragg reflection is observed and the body-centered condition ($h + k + l = 2n$) is still fulfilled at low temperature. Therefore, the C_{60} orientational ordering does not affect the body-centering. To get more information, new four-circle diffraction experiments have been carried out at 123 K and 110 K. The data collection and analysis are summarized in references [29,30] and will be described in detail elsewhere [23]. The results which are specifically related to the reduction of the disorder are already presented here. Figure 6 shows a schematic representation of a simple orientational order/disorder model. At room temperature, one considers two randomly distributed C_{60} orientations (corresponding to angles φ and $\pi/2 + \varphi$ around \mathbf{c} , see Fig. 6a) within the space group $I4/m$. The C_{60} molecule does not possess any 4-fold symmetry axis and the orientational ordering must thus lead to a lower symmetry. In Figure 6b, the C_{60} ordering is schematized in the space group $I2/m$. In order to preserve the point symmetry operations at the macroscopic level, there must be two types of orientational domains, in which all molecules have the same orientation angle φ or $\pi/2 + \varphi$. At 123 K, attempts to refine the structure within the $I2/m$ hypothesis fail (the refinement diverges). Within the $I4/m$ hypothesis, a good reliability factor $R = 0.051$ is obtained from the structural refinement. At 110 K, structural refinements within the $I4/m$ and $I2/m$ hypotheses give reliability factors $R = 0.082$ and 0.037 respectively. The low R value for $I2/m$ and the significant difference from that for $I4/m$ validate the $I2/m$ hypothesis [31]. It follows that a structural phase transition from $I4/m$ to $I2/m$ space groups takes place between 123 K and 110 K in C_{60} -tetraphenylphosphonium bromide. This transition appears to be mainly related to the suppression of the on-site orientational disorder

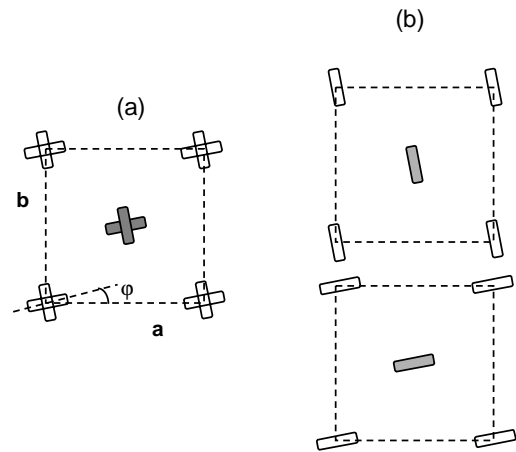


Fig. 6. Schematic view of the C_{60} orientations for the (a) $I4/m$ and (b) $I2/m$ space groups. The bars indicate the orientation of the molecules (angles φ or $\pi/2 + \varphi$ with respect to axis \mathbf{a}); they represent the projection onto the (\mathbf{a}, \mathbf{b}) plane of the C_1-C_2 bond in Figure 1. Shaded (open) bars represent molecules at $z = 0$ ($z = 1/2$).

of the C_{60} molecules, as illustrated in Figure 6. Indeed, the value of the C_{60} orientation angle ($\varphi \approx 10^\circ$) and the phenyl ring orientations or the phosphor or halide positions are roughly the same at 293 K, 123 K and 110 K. At room temperature, minimization of the energy between the tetraphenylphosphonium and the fulleride ions is attributed to face-to-face and edge-to-face interactions between the phenyl rings and the fullerides [11,22], which are preserved in the low temperature $I2/m$ structure.

In the ordered $I2/m$ phase, direct observation of a static Jahn-Teller distortion may be measurable, more easily than when there is orientational disorder. Actually, some dispersion is found between the molecular diameters deduced from the atomic positions (minimum diameter of 7.057(8) Å and maximum diameter of 7.124(11) Å), but no clear symmetry breaking of the C_{60} molecule is observed, while axial elongation or contraction have been evidenced in $[PPN^+]_2C_{60}^{2-}$ or in decamethylnickelocenium buckminsterfulleride [7,8]. Therefore, the currently available structure refinements are not sensitive enough to determine the C_{60} distortion, probably very weak, resulting from the Jahn-Teller effect in C_{60} -tetraphenylphosphonium bromide.

3 Discussion

In this section, we discuss our structural results in relation with the ESR [14,23] and infrared [20] data and with the Jahn-Teller effect.

We have shown that the diffuse scattering observed at room temperature can be reasonably attributed to C_{60} orientational disorder. However, its intensity modulations cannot be fully explained considering only the two-orientation disorder deduced from the Bragg peak

intensity analyses in references [10,11]. The disorder is probably more complex and it may involve several orientational configurations. Further studies should clarify this important aspect. The diffuse scattering, related to the differences between the structure factors of the molecules with different orientations (Eq. (2)), appears as a more sensitive probe to the complete C₆₀ orientational disorder than the Bragg scattering, which is related to the mean value of the structure factors. Note that a structural model different from that of references [10,11] has been proposed in reference [32]. This model considers that the C₆₀ molecules are ordered at room temperature which is invalidated by our diffuse scattering observations.

Aside from this broad diffuse scattering, there is a clear evidence for weak diffuse lines running along directions of the type $\mathbf{a}^* + \mathbf{c}^*$ and $\mathbf{b}^* + \mathbf{c}^*$. They correspond to some kind of disorder involving (101) and (011) planes, which are homopolar. The exact nature of this disorder is still unclear but the geometry of the diffuse scattering evidences a two-dimensional character of the compound.

Although the disorder model with two C₆₀ orientations (φ and $\pi/2 + \varphi$) described within the space group I4/m does not account correctly for the room temperature diffuse scattering distribution, it can be considered as a useful approach for the analysis of the low temperature behavior. The strong decrease of the diffuse scattering modulations between room temperature and 110 K (the measured temperature being underestimated) indicates some C₆₀ orientational ordering. We have found that simultaneously the average structure changes from I4/m to I2/m so that this ordering corresponds to the formation of two types of orientational domains, with either the φ or $\pi/2 + \varphi$ molecular orientations. A phase transition thus occurs in the 110–120 K range. Correlatively, far-infrared studies in C₆₀-tetraphenylphosphonium iodine had indicated a weak transition in the 125 K–150 K region, for both the C₆₀⁻ and counterion modes [20], while no transition had been evidenced by previous X-ray diffraction nor by differential scanning calorimetry measurements [11(b),17].

Isostructural C₆₀-tetraphenylphosphonium salts with bromine (X = Br) and iodine (X = I) have been investigated by ESR spectroscopy [14,23]. Perpendicularly to the \mathbf{c} axis, a splitting of the Landé factor g of the C₆₀⁻ molecule into two components g_{\perp} and g_{\parallel} ($g_{\perp} > g_{\parallel}$) has been evidenced below $T_1 \sim 120$ K for X = Br and $T_1 \sim 140$ K for X = I [14]; the third component, along the \mathbf{c} axis, is equal to g_{\parallel} [23]. The splitting differentiates one axis in the (\mathbf{a} , \mathbf{b}) plane from the perpendicular axis in the (\mathbf{a} , \mathbf{b}) plane and from the \mathbf{c} axis. It increases with decreasing temperature below T_1 and it saturates around 60 K. The Landé factor splitting appears as the signature for a Jahn-Teller distortion. Far-infrared study of C₆₀-tetraphenylphosphonium iodide have also shown a splitting of some F_{1u} modes into doublets at room temperature, indicating a Jahn-Teller effect [20]. Note that ESR gives indications for a Jahn-Teller effect below T_1 only, while infrared data show that it is already present at room temperature. The following scenario has thus been proposed in reference [20]. At room

temperature, there would be a dynamic competition between different Jahn-Teller distortions (occurring between distortions of the same symmetry, along different molecular directions, or between distortions of different symmetries, since they are nearly degenerate in energy [4]). FIR frequencies being of the order of 10^{13} s⁻¹ and ESR being sensitive to frequencies below 10^9 s⁻¹, the Jahn-Teller distortions would have been observed in FIR experiments while they were averaged out in ESR experiments.

Our X-ray diffuse scattering and diffraction results point toward a C₆₀ orientational ordering phase transition around 120 K in C₆₀-tetraphenylphosphonium bromide. It occurs in the same temperature range as the Landé factor splitting in ESR data, indicating a possible common origin. Furthermore, that the Landé factor anisotropy varies as an order parameter [14] supports the common origin hypothesis. The C₆₀ orientational ordering, which is a *bulk* phenomenon, appears correlated with the *molecular* Jahn-Teller effect [20]. This may be explained as follows: the Jahn-Teller distortion can be stabilized at the structural transition due to crystal field effects [33]. Indeed, at the orientational ordering transition, the crystal field symmetry on the molecule is lowered from 4/m to 2/m, which may induce the static stabilization of a Jahn-Teller distortion of a given symmetry along a specific molecular axis. Correlatively, in solutions, polar solvent can lower the symmetry more than non-polar ones, which suggests dynamic Jahn-Teller effects trapped in static structures by the environment [34].

The diffuse scattering and diffraction results on C₆₀-tetraphenylphosphonium bromide have pointed toward a C₆₀ ordering at low temperature, which can be correlated with the static stabilization of the molecular Jahn-Teller effect. Further diffraction experiments below 60 K, where the Landé factor splitting saturates, are also awaited to try measuring directly the fulleride Jahn-Teller distortion. Note that in numerous C₆₀-based compounds, the nearly spherical C₆₀ molecule can exhibit many orientational ordering phenomena and that the Jahn-Teller effect is expected to play an important role in electronic properties. Other studies of the stabilization of Jahn-Teller distortions, in relation with orientational ordering, would thus be very interesting.

We thank P. Batail and K. Boubekeur for the use of their diffractometer and V. Long for providing us with her preprint before publication.

References

1. M.J. Rosseinsky, *Chem. Mater.* **10**, 2665 (1998).
2. P.-M. Allemand, K.C. Khemani, A. Koch, F. Wudl, K. Holczer, S. Donovan, G. Grüner, J.D. Thompson, *Science* **253**, 301 (1991).
3. V. de Coulon, J.L. Martins, F. Reuse, *Phys. Rev. B* **45**, 13671 (1992).

4. N. Koga, K. Morokuma, Chem. Phys. Lett. **196**, 191 (1992).
5. J. Ihms, Phys. Rev. B **49**, 10726 (1994).
6. M. Lannoo, G.A. Baraff, M. Schlüter, D. Tomanek, Phys. Rev. B **44**, 12106 (1991); A. Auerbach, N. Manini, E. Tosatti, Phys. Rev. B **49**, 12998 (1994); N. Manini, E. Tosatti, A. Auerbach, Phys. Rev. B **49**, 13008 (1994); W. Victoroff, M. Héritier, J. Phys. I France **6**, 2175 (1996); T. Kawamoto, Solid State Commun. **101**, 231 (1997).
7. P. Paul, Z. Xie, R. Bau, P.D.W. Boyd, C.A. Reed, J. Am. Chem. Soc. **116**, 4145 (1994).
8. W.C. Wan, X. Liu, G.M. Sweeney, W.E. Broderick, J. Am. Chem. Soc. **117**, 9580 (1995).
9. P.-M. Allemand, G. Srdanov, A. Koch, K. Khemani, F. Wudl, Y. Rubin, F. Diederich, M.M. Alvarez, S.J. Anz, R.L. Whetten, J. Am. Chem. Soc. **113**, 2780 (1991). The proposed formulation for C₆₀-tetraphenylphosphonium was [Ph₄P]₃[C₆₀][hal]₂ instead of [Ph₄P]₂[C₆₀][hal] (hal = hallogene). It was used in references [13, 16, 18].
10. A. Pénicaud, A. Pérez-Benítez, R. Gleason, E. Muñoz, R. Escudero, J. Am. Chem. Soc. **115**, 10392 (1993).
11. (a) U. Bilow, M. Jansen, J. Chem. Soc., Chem. Commun. **4**, 403 (1994); (b) U. Bilow, M. Jansen, Z. Anorg. Allg. Chem. **621**, 982 (1995).
12. W. Schütz, J. Gmeiner, A. Schilder, B. Gotschy, V. Enkelmann, J. Chem. Soc., Chem. Commun. **13**, 1571 (1996).
13. U. Becker, G. Denninger, V. Dyakonov, B. Gotschy, H. Klos, G. Rösler, A. Hirsch, H. Winter, Europhys. Lett. **21**, 267 (1993).
14. B. Gotschy, M. Keil, H. Klos, I. Rystau, Solid State Commun. **92**, 935 (1994).
15. A. Pénicaud, A. Pérez-Benítez, R. Escudero, C. Coulon, Solid State Commun. **96**, 147 (1995).
16. G. Völkel, A. Pöppl, J. Simon, J. Hoentsch, S. Orlinskii, H. Klos, B. Gotschy, Phys. Rev. B **52**, 10188 (1995).
17. B. Gotschy, G. Völkel, J. App. Magn. Res. **11**, 229 (1996).
18. V. Dyakonov, G. Rösler, H. Klos, B. Gotschy, G. Denninger, A. Hirsch, Synthetic Metals **55-57**, 3214 (1993).
19. V.N. Semkins, N.G. Spitsina, S. Król, A. Graja, Chem. Phys. Lett. **256**, 616 (1996).
20. V.C. Long, J.L. Musfeldt, K. Kamarás, A. Schilder, W. Schütz, Phys. Rev. B **58**, 14338 (1998).
21. M. Polomska, J.-L. Sauvajol, A. Graja, A. Girard, Solid State Commun. **111**, 107 (1999).
22. M. Scudder, I. Dance, J. Chem. Soc., Dalton Trans. **19**, 3155 (1998).
23. A. Pénicaud *et al.*, in preparation.
24. A. Guinier, *Théories et techniques de la radiocristallographie* (Dunod, Paris, 1956); A. Guinier, *X-ray Diffraction in Crystals and Amorphous Bodies* (Dover publications, Inc., 1994); E. Warren, *X-ray diffraction* (Addison-Wesley: Reading, MA, 1969); reproduced by Dover, New-York, 1990.
25. R. Moret, P. Launois, S. Ravy, M. Julier, J.M. Godard, Synthetic Met. **86**, 2327 (1997).
26. J.R.D. Copley, D.A. Neumann, R.L. Cappelletti, W.A. Kamitakahara, J. Phys. Chem. Solids **53**, 1353 (1992).
27. R. Moret, S. Ravy, J.M. Godard, J. Phys. I France **2**, 1699 (1992); *ibid* **3**, 1085 (1993).
28. P. Launois, S. Ravy, R. Moret, Phys. Rev. B **52**, 5414 (1995).
29. Data collection at 123 K: ENRAF NONIUS CAD4, Mo K α , 1947 independent reflections, 1358 with $I > 3\sigma(I)$, refinement [30] in I4/m with 145 parameters, $R = 0.051$, $Rw = 0.048$, residual densities: +0.41 and $-1.36 \text{ e}/\text{\AA}^3$. Data collection at 110 K: Image plate STOE IPDS, Mo K α , 1914 independent reflections, 1409 with $I > 3\sigma(I)$. Refinement in I2/m with 258 parameters, $R = 0.037$, $Rw = 0.039$, residual densities: +0.4 and $-0.24 \text{ e}/\text{\AA}^3$. Refinement in I4/m with 144 parameters, $R = 0.082$, $Rw = 0.101$, residual densities: +0.76 and $-1.74 \text{ e}/\text{\AA}^3$.
30. Program used for the structure refinement: CRYSTALS issue 10 (1996), D.J. Watkin, C.K. Prout, J.R. Carruthers, P.W. Betteridge; CAMERON (1996), D.J. Watkin, C.K. Prout, L.J. Pearce, Chem. Crystall. Lab. (Oxford, UK).
31. Note that the I2/m group is monoclinic and not quadratic like I4/m, but that no deviations from the quadratic symmetry have been found on the unit cell parameters. For a C₆₀ ordering transition like that illustrated in Figure 6, deviations are expected to be very small due to the rather homogeneous distribution of the C atoms on the molecule.
32. V.V. Gritsenko, G.A. Dyachenko, G.V. Shilov, N.G. Spitsyna, E.B. Yagubskii, Russian Chem. Bull. **46**, 1878 (1997).
33. I.B. Bersucker, *The Jahn-Teller Effect and Vibronic Interactions in Modern Chemistry* (Plenum, New York, 1984).
34. C.A. Reed, R.D. Bolskar, Chem. Rev. **100**, 1075 (2000).